



OPEN

SUBJECT AREAS:  
GEOCHEMISTRY  
GEOLOGYReceived  
30 December 2013Accepted  
22 April 2014Published  
3 June 2014Correspondence and  
requests for materials  
should be addressed to  
X.-L.W. (wxl@nju.edu.  
cn) or G.-F.X. (njxgfu@  
163.com)

# Diversity in early crustal evolution: 4100 Ma zircons in the Cathaysia Block of southern China

Guang-Fu Xing<sup>1</sup>, Xiao-Lei Wang<sup>2,3</sup>, Yusheng Wan<sup>4</sup>, Zhi-Hong Chen<sup>1</sup>, Yang Jiang<sup>1</sup>, Kouki Kitajima<sup>3</sup>,  
Takayuki Ushikubo<sup>3</sup> & Phillip Gopon<sup>3</sup>

<sup>1</sup>Nanjing Institute of Geology and Mineral Resources, China geological survey, Nanjing 210016, PR China, <sup>2</sup>State Key Laboratory for Mineral Deposits Research, School of Earth Science and Engineering, Nanjing University, Nanjing 210093, China, <sup>3</sup>WiscSIMS, Department of Geoscience, University of Wisconsin, 1215 W Dayton Street, Madison, WI 53706, USA, <sup>4</sup>Beijing SHRIMP Center, Institute of Geology, Chinese Academy of Geological Sciences, Beijing 100037, China.

Zircons are crucial to understanding the first 500 Myr of crustal evolution of Earth. Very few zircons of this age (>4050 Ma) have been found other than from a ~300 km diameter domain of the Yilgarn Craton, Western Australia. Here we report SIMS U-Pb and O isotope ratios and trace element analyses for two ~4100 Ma detrital zircons from a Paleozoic quartzite at the Longquan area of the Cathaysia Block. One zircon (<sup>207</sup>Pb/<sup>206</sup>Pb age of 4127 ± 4 Ma) shows normal oscillatory zonation and constant oxygen isotope ratios (δ<sup>18</sup>O = 5.8 to 6.0‰). The other zircon grain has a ~4100 Ma magmatic core surrounded by a ~4070 Ma metamorphic mantle. The magmatic core has elevated δ<sup>18</sup>O (7.2 ± 0.2‰), high titanium concentration (53 ± 3.4 ppm) and a positive cerium anomaly, yielding anomalously high calculated oxygen fugacity (FMQ + 5) and a high crystallization temperature (910 °C). These results are unique among Hadean zircons and suggest a granitoid source generated from dry remelting of partly oxidizing supracrustal sediments altered by surface waters. The ~4100 Ma dry melting and subsequent ~4070 Ma metamorphism provide new evidence for the diversity of the Earth's earliest crust.

The Earth's earliest history is poorly known because of the lack of rocks from its first 500 m.y. (i.e., >4050 Ma). The mafic rocks from the Nuvvuagittuq greenstone belt of the Superior Craton, Canada, produced a short-decay Nd isotope isochron age of ~4300 Ma<sup>1</sup>. However, the <sup>146</sup>Sm-<sup>142</sup>Nd values might represent early mantle inheritance and the rock age may be as young as ~3800 Ma<sup>2</sup>. Zircon (ZrSiO<sub>4</sub>), due to its robust chemical and physical features, may be the only common accessory mineral in continental rocks that could survive the extreme conditions of Earth's early evolution. Rare Hadean-Early Archean zircons are important for understanding the formation of Earth's protocrust and ocean<sup>3,4</sup>, the characteristics of primordial mantle<sup>5</sup>, and continental weathering<sup>6</sup>. Although still debated<sup>7-9</sup>, a number of isotopic observations have suggested that the Hadean Earth may have had a relatively stable, basaltic crustal lid, without plate recycling analogous to modern-style plate tectonics<sup>5,10-13</sup>.

It should be noted that our knowledge of early earth crustal evolution has mostly been based on studies of zircons found in Archean metasedimentary rocks in Western Australia (dominantly the Jack Hills)<sup>3,4,14-17</sup>. Is this an accident of preservation or was this area unique in the Hadean eon? We are aware of only four > 4050 Ma zircons analyzed by SIMS (secondary ion mass spectrometer) that have been reported as detritus and xenocrysts outside Western Australia: one in the Itsaq Gneiss complex of West Greenland (4079 ± 18 Ma)<sup>18</sup>, one in the Acasta Gneiss of Northwest Territories, Canada (4189 ± 46 Ma)<sup>19</sup> and two in China (one in western Tibet, 4103 ± 4 Ma; and one in the North Qinling Belt, 4080 ± 9 Ma)<sup>20,21</sup>. There is only one *in situ* ion microprobe analysis for each of these four zircons and, although they show concordant U-Th-Pb isotopic ages (concordance > 90%), these ages have not been reproduced. These rare survivors from outside Western Australia need careful and comprehensive investigations by a wide range of methods to establish their origins and to help understand the diversity of the earliest crustal evolution of the Earth. In this work, we report SIMS analyses of two > 4050 Ma zircon xenocrysts from one quartzite sample in the Cathaysia Block of southern China. Their oxygen isotope ratios and trace elements (especially Ti concentrations) provide new evidence for the diversity of earliest continental crust.



**Geological setting.** Southern China (*i.e.*, the South China Block) is composed of the Yangtze Block to the northwest and the Cathaysia Block to the southeast (Fig. 1a). The Cathaysia Block is dominated by Early Paleozoic metamorphic rocks and Mesozoic granitoids, and volcanic-sedimentary rocks, with minor Precambrian rocks (including Neoproterozoic 970–750 Myr volcanic-sedimentary rocks and rare Paleoproterozoic gneissic metamorphic rocks). Zircon crystals of this study were separated from a quartzite within the Longquan Group paragneiss that was originally deposited after 700 Ma and metamorphosed at  $\sim 450$  Ma at the Longquan area of southwestern Zhejiang Province in the Cathaysia Block (Fig. 1b, Supplementary Figs. DR1–2).

## Results

Two zircon grains (#8 and #123) with  $^{207}\text{Pb}/^{206}\text{Pb}$  ages older than 4050 Ma were found among 235 U–Pb analyses on 214 zircons from the quartzite sample. Grain #8 shows complicated zoning in CL with an oscillatory-zoned magmatic core surrounded by an intermediate CL-intensity unzoned metamorphic mantle ( $\text{Th}/\text{U} \leq 0.05$ ) and two main outermost unzoned overgrowths (one dark and one bright in CL; Fig. 2a; Supplementary Fig. DR3). In addition, there is a bright unzoned domain in the lower right of the core, showing crosscutting relations with other domains of the core in CL (Fig. 2a; Fig. DR3), possibly representing an altered domain. This is supported by the low  $\text{Th}/\text{U}$  (0.06) and high  $\delta^{18}\text{O}$  (see below). In contrast, grain #123 shows a simple texture in CL, with dark and bright oscillatory zones surrounding an unzoned (possibly radiation damaged) core (Fig. 2b; Fig. DR3).

The results of the two dating sessions are consistent, suggesting the core (pit #s U8.1, U8.8, U8.10) and metamorphic mantle (#s U8.3, U8.7) of grain #8 are nearly concordant ( $\geq 95\%$  concordance except #U8.10; Table 1) and formed in the ranges 4150–4100 Ma and 4070–4060 Ma respectively (Fig. 2a). The altered domain of grain #8 core

gives a  $^{207}\text{Pb}/^{206}\text{Pb}$  age of  $4121 \pm 7$  Ma ( $1\sigma$ ; 98% concordance), indistinguishable from other core analyses. In addition, the two outermost pits in the overgrowths of this grain were dated at  $3843 \pm 7$  Ma ( $1\sigma$ ) and  $3679 \pm 6$  Ma ( $1\sigma$ ) respectively (#U8.6 and #U8.9 in Fig. 2a; Fig. DR3m). For grain #123, nine analyses (5 of 9 with concordance  $> 89\%$ ) from the oscillatory region show  $^{207}\text{Pb}/^{206}\text{Pb}$  ages in the range 4130–4030 Ma (Table 1; Fig. 2b), and the unzoned core gives a younger  $^{207}\text{Pb}/^{206}\text{Pb}$  age of  $3956 \pm 8$  Ma ( $1\sigma$ ) (82% concordance; #U123.7; Table 1; Fig. 2b; Fig. DR3n).

Four oxygen isotope analyses in the concordant domain of the core of grain #8 give identical results (Fig. DR3g; Supplementary Table S1), yielding an average  $\delta^{18}\text{O}$  of  $7.2 \pm 0.2\text{‰}$  ( $n = 4$ , 2SD). The metamorphic mantle of grain #8 yielded an average  $\delta^{18}\text{O}$  of  $8.0 \pm 0.7\text{‰}$  ( $n = 4$ , 2SD), which is similar to the altered domain in the core ( $\delta^{18}\text{O} = 7.9 \pm 0.2\text{‰}$ , #O8.3; Table S1). The ca. 3840 and 3780 Ma outermost overgrowths yield similar  $\delta^{18}\text{O}$  values (7.6‰ vs. 7.4‰; Table S1; #O8.9, #O8.11 in Fig. DR3g). In contrast, grain #123 shows consistent and mantle-like oxygen isotope ratios in its magmatic zones ( $\delta^{18}\text{O} = 5.9 \pm 0.2\text{‰}$ , 2SD,  $n = 6$ ), and the unzoned damaged core gives similar  $\delta^{18}\text{O}$  of  $5.6 \pm 0.2\text{‰}$  (#O123.1; Table S1; Fig. DR3h).

The magmatic areas (including the core of #8 and zoned domains of #123) of both grains show a positive slope for chondrite-normalized rare earth element (REE) profiles with significant positive Ce anomalies and negative Eu anomalies (Supplementary Table S2; Fig. 3). They are geochemically similar to pristine continental zircons on Earth in their high  $(\text{Sm}/\text{La})_{\text{N}}$  and  $\text{U}/\text{Yb}$  ratios (Fig. 4). Two analyses from the core of grain #8 showed the highest [Ti] (Ti concentration) (51.5 and 54.0 ppm). The zoned domains of #123 gave relatively low [Ti] (19.8 ppm for dark zonation and 14.7 ppm for light zonation in CL; Table S2). The altered domain and the metamorphic mantle/rim of grain #8 show similar REE patterns, with relatively low REE abundances and weakly negative Eu anomalies

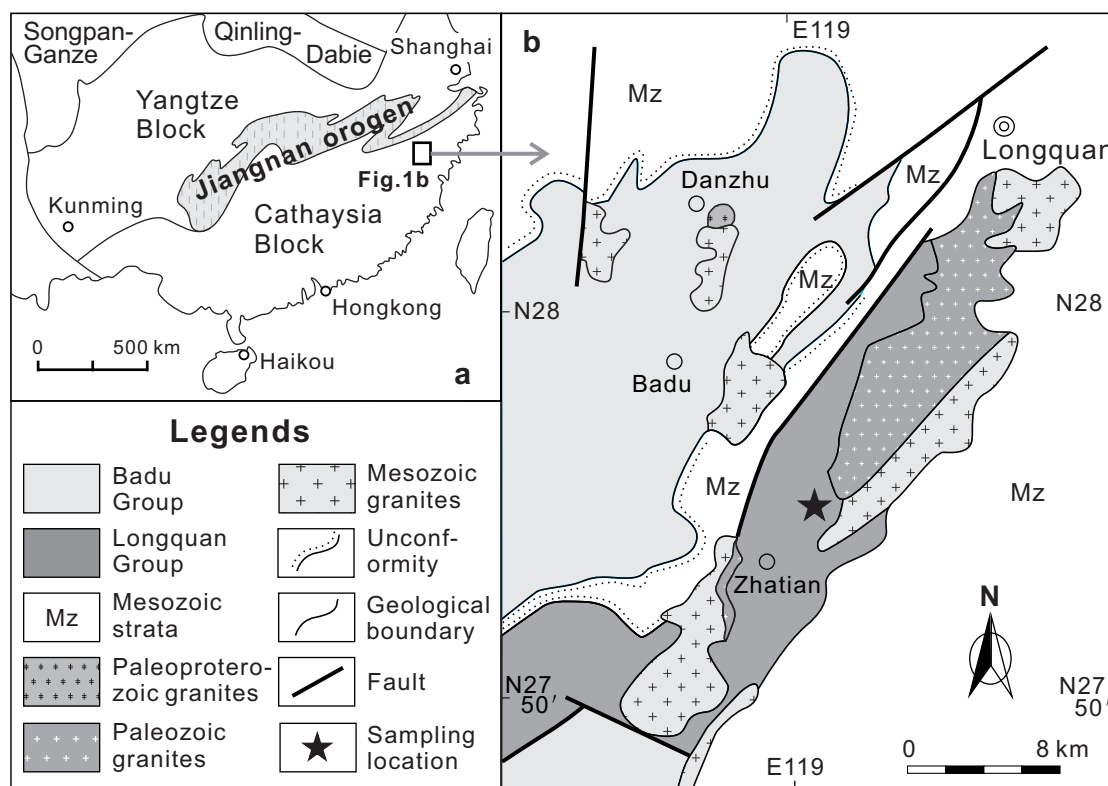


**Figure 1** | Geological sketch map showing the sampling location of the two ancient zircon grains. (a) Southern China composed of the Yangtze and Cathaysia blocks and the Jiangnan orogen between them; (b) Longquan area, southwestern Zhejiang Province. This map image was made by the co-authors Jiang Yang and Xing Guangfu according to their geological survey work, using the software Mappgis and CorelDraw.

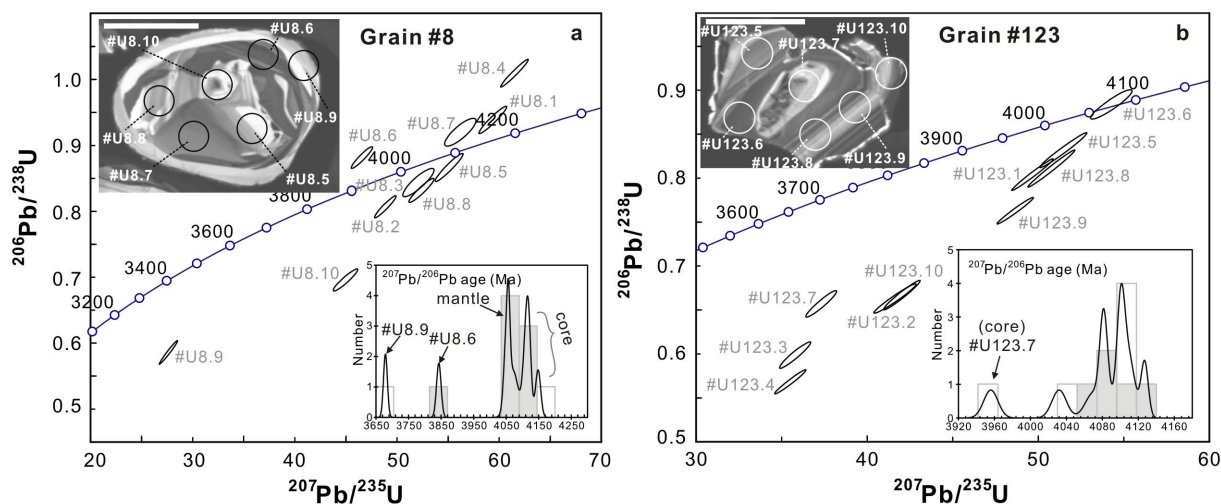


**Figure 2** | U-Pb Concordia plots for the two ancient zircons. The CL image (before the second session of U-Pb dating) and age histogram for each grain is also indicated for each grain as insets. The gray filled columns in the lower right insets represent the analyses with concordance > 88%, while the open ones are < 88% concordance analyses. Error ellipses are shown in  $1\sigma$ .

(Fig. 3). They also show similar [Ti] (15.3 ppm versus 23.0–18.8 ppm; Table S2).

## Discussion

All of the analyses ( $n = 18$ ) of the two U-Pb sessions show  $^{207}\text{Pb}/^{206}\text{Pb}$  ages older than 3950 Ma, with the exception of the above-mentioned two outermost overgrowths of grain #8 (#U8.6 and #U8.9 in Fig. 2a). Twelve of the eighteen > 3950 Ma analyses show concordance better than 89% (Table 1). Thus the  $^{207}\text{Pb}/^{206}\text{Pb}$  ages are not significantly affected by Pb mobilization<sup>22</sup> that might lead to anomalously lower or elevated  $^{207}\text{Pb}/^{206}\text{Pb}$  ages in some parts of a zircon at the expense of other domains. Four analyses (#s U8.1, U8.4, U8.6 and 8.7) show reverse discordance (Fig. 2a). Most of these analyses are from or overlap the low-Th/U metamorphic mantle of grain #8. The reverse discordance may have resulted from localized Pb mobility within partly radiation damaged zircons. The consistency of  $^{207}\text{Pb}/^{206}\text{Pb}$  ages and good concordance of the analyses suggest that  $^{207}\text{Pb}/^{206}\text{Pb}$  ages with uncertainties lower than 15 m.y. ( $1\sigma$ ) give reliable ages that are the oldest known for zircons from southern China.

High-grade regional metamorphism likely accompanied the formation of the earliest granitic rocks on Earth due to heating from the underplating mantle magmas and high geothermal gradient at that time, although radiogenic heat production is also suggested as a mechanism for crustal melting<sup>11</sup>. However, such metamorphic rocks have not been identified and may not have survived. Metamorphic zircon can potentially provide a record of the early Earth metamorphism and help understand the crustal evolution of Earth.

Metamorphic zircons can commonly be distinguished from igneous zircons by their low Th/U ratios (generally < 0.07<sup>23</sup>), the absence of oscillatory zonation in CL<sup>24</sup>, and weak to absent negative Eu anomalies<sup>23</sup>. The magmatic core of grain #8 is surrounded by a mantle with intermediate CL-intensity that is unzoned (Fig. DR3). Four analyses (trace elements #TE8.3, #TE8.4 and #U8.3, #U8.7) in the mantle all gave Th/U ratios  $\leq 0.05$  (Table 1 and Table S2), suggesting that the unzoned layer (i.e. the mantle of grain #8) is metamorphic in origin. Hadean to Early Archean analyses with low Th/U (< 0.07) ratios have been sporadically reported in detrital zircons from Jack Hills. Cavosie et al.<sup>25</sup> reported one analysis ( $^{207}\text{Pb}/^{206}\text{Pb}$  age of  $4062 \pm 10$  Ma, #22-2 of sample 01JH65) with Th/U ratio of 0.04. Unfortunately, this grain was removed during later polishing. Similarly, Harrison et al.<sup>9</sup> showed one low Th/U (0.05) analysis ( $^{207}\text{Pb}/^{206}\text{Pb}$  age of  $4046 \pm 12$  Ma, #RSES43-5.7) without detailed oxygen isotopes and CL images. The 4070–4060 Ma metamorphic

mantle surrounding the magmatic core of grain #8 shows low Th/U ratio (average 0.04; #U8.7, #TE8.3, #TE8.4; Table 1 and Table S2). Four oxygen isotope analyses (#s O8.1, O8.5, O8.6 and O8.8) in this metamorphic zone gave  $\delta^{18}\text{O}$  ranging from 7.6‰ to 8.3‰ (Table S1), with a mean value of  $8.0 \pm 0.7\text{‰}$ , which is a little higher than that ( $7.2 \pm 0.2\text{‰}$ ) of the magmatic core. The slightly elevated oxygen isotope ratios suggest the existence of  $^{18}\text{O}$ -enriched fluids that sourced from low-temperature supracrustal processes. It possibly represents the oldest known metamorphic event on Earth documented by zircon accompanied by reliable CL images, oxygen isotope and trace element analyses.

The titanium-in-zircon thermometer<sup>26,27</sup> (also see the equation (1) in the supplementary files) has been widely applied to magmatic zircons. Although the meaning of calculated temperatures and the mechanism of Ti in zircon are still unclear<sup>28–32</sup>, comparison based on same assumptions can be an effective way to evaluate early crustal evolution<sup>33</sup>. Most of the Jack Hills analyses (free of cracks) contain less than 20 ppm titanium based on published data (Fig. 5), yielding an average calculated temperature of  $697 \pm 47^\circ\text{C}$  (1SD,  $n = 50$ ; Table S3) assuming unit activities of  $\text{TiO}_2$  and  $\text{SiO}_2$  and applying no pressure correction (same assumption below). The mean value is consistent with the result ( $696 \pm 33^\circ\text{C}$ ) by Watson and Harrison<sup>26</sup> and their updated value ( $682 \pm 26^\circ\text{C}$ )<sup>4</sup>. A few Jack Hills zircons also show temperatures higher than  $800^\circ\text{C}$  due to their high [Ti]<sup>34</sup>, but no detailed CL and/or BSE images were provided along with [Ti] to help evaluate whether the [Ti] analyses had been affected by the existences of micro-cracks and/or inclusions<sup>8,34–36</sup>.

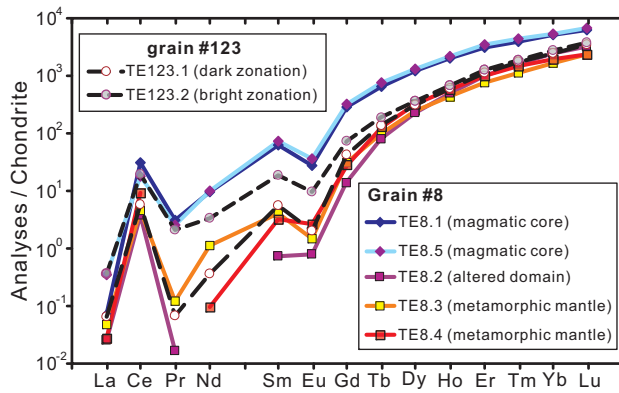
The calculated low temperature for Jack Hills zircons was suggested to correspond to the temperature of wet minimum melting in present-day crust<sup>26,34</sup>. However, two analyses (#TE8.1 and #TE8.5) of the magmatic core of grain #8 give consistent [Ti], with a mean value of  $53 \pm 3.4$  ppm, corresponding to a temperature of  $910^\circ\text{C}$  by titanium-in-zircon thermometer. This is the highest reported value for a Hadean zircon from Earth (Fig. 5) with detailed CL and oxygen isotopes, and it may also represent one of the highest values of [Ti] in terrestrial zircons from any time period<sup>29,32,35,37</sup>. Interestingly, the metamorphic mantle of grain #8 and the analyses in grain #123 show uncorrected Ti-in-zircon temperatures ( $776\text{--}820^\circ\text{C}$ ; Table S2) higher than many of the published Hadean zircons from Jack Hills. Further imaging has shown that no tiny cracks occur in the analyzing pits to provide additional [Ti] and the consistency of [Ti] of different pits in the core of grain #8 precludes the result of non-Henry's law behavior in the incorporation of Ti in zircon. Therefore, the high-



Table 1 | SHRIMP U-Th-Pb isotopic data for two old zircon grains of southern China

Spot	% $^{206}\text{Pb}_c$	U (ppm)	Th (ppm)	Th/U	$^{206}\text{Pb}^*$ (ppm)	$^{207}\text{Pb}^*/^{206}\text{Pb}^*$	$^{207}\text{Pb}^*/^{235}\text{U}$	$^{206}\text{Pb}^*/^{238}\text{U}$	Con. %	$^{207}\text{Pb}^*/^{206}\text{Pb}^*$ Age (Ma)	$^{207}\text{Pb}^*/^{235}\text{U}$ Age (Ma)	$^{206}\text{Pb}^*/^{238}\text{U}$ Age (Ma)
Session 1												
#U8.1	0.03	286	146	0.53	230	0.4591 ± 22	59.4 ± 0.9	0.939 ± 14	104	4115 ± 7	4164 ± 15	4267 ± 46
#U8.2	0.04	364	66	0.19	253	0.4392 ± 20	48.9 ± 0.7	0.807 ± 11	94	4049 ± 7	3970 ± 15	3815 ± 41
#U8.3	0.02	635	33	0.05	460	0.4477 ± 41	52.1 ± 1.0	0.844 ± 14	97	4077 ± 14	4033 ± 9	3945 ± 48
#U8.4	0.01	350	50	0.15	303	0.4415 ± 15	61.5 ± 0.9	1.010 ± 14	111	4057 ± 5	4199 ± 15	4501 ± 46
#U123.1	0.07	534	100	0.19	369	0.4486 ± 13	49.7 ± 0.8	0.804 ± 12	93	4081 ± 4	3987 ± 16	3802 ± 44
#U123.2	0.03	495	148	0.31	284	0.4581 ± 19	42.1 ± 0.7	0.667 ± 11	80	4112 ± 6	3822 ± 17	3294 ± 42
#U123.3	0.07	678	154	0.23	350	0.4342 ± 23	35.9 ± 0.6	0.599 ± 10	75	4032 ± 8	3663 ± 17	3026 ± 40
#U123.4	0.05	926	136	0.15	452	0.4543 ± 16	35.6 ± 0.6	0.5684 ± 9	71	4099 ± 5	3656 ± 16	2901 ± 36
Session 2												
#U8.5	0.01	273	17	0.06	203	0.4611 ± 23	55.1 ± 0.9	0.867 ± 14	98	4121 ± 7	4089 ± 16	4023 ± 47
#U8.6	0.00	604	29	0.05	458	0.3829 ± 18	46.6 ± 0.7	0.882 ± 11	106	3843 ± 7	3921 ± 14	4075 ± 40
#U8.7	0.02	417	22	0.05	329	0.4432 ± 44	56.2 ± 1.0	0.920 ± 14	103	4063 ± 15	4109 ± 18	4204 ± 46
#U8.8	0.00	274	134	0.51	196	0.4568 ± 25	52.4 ± 0.8	0.832 ± 12	95	4107 ± 8	4038 ± 16	3901 ± 43
#U8.9	0.01	393	42	0.11	198	0.3435 ± 14	27.7 ± 0.6	0.586 ± 12	81	3679 ± 6	3410 ± 20	2972 ± 47
#U8.10	0.00	225	136	0.62	134	0.4694 ± 26	45.0 ± 0.8	0.696 ± 11	82	4148 ± 8	3888 ± 17	3404 ± 41
#U123.5	0.01	388	79	0.21	278	0.4492 ± 15	51.5 ± 0.9	0.832 ± 13	96	4083 ± 5	4022 ± 17	3903 ± 48
#U123.6	0.02	601	103	0.18	457	0.4454 ± 26	54.3 ± 0.8	0.884 ± 11	100	4070 ± 9	4075 ± 15	4084 ± 40
#U123.7	0.04	327	144	0.45	184	0.4127 ± 22	37.4 ± 0.6	0.657 ± 10	82	3956 ± 8	3703 ± 16	3255 ± 39
#U123.8	0.01	427	107	0.26	297	0.4547 ± 12	50.8 ± 0.9	0.811 ± 14	93	4101 ± 4	4009 ± 17	3828 ± 49
#U123.9	0.01	461	130	0.29	303	0.4628 ± 13	48.7 ± 0.7	0.763 ± 10	89	4127 ± 4	3966 ± 14	3656 ± 38
#U123.10	0.14	317	100	0.33	181	0.4559 ± 20	41.7 ± 0.8	0.663 ± 11	80	4105 ± 6	3812 ± 18	3280 ± 44

\*common lead corrected by  $^{206}\text{Pb}$ .  
 $\%^{206}\text{Pb}_c$  is  $[\text{common } ^{206}\text{Pb}/\text{total } ^{206}\text{Pb}] \times 100$ .  $^{206}\text{Pb}^*$  means the concentration of radiogenic lead. Con. % is percentage concordance of defined as  $(^{206}\text{Pb}^*/^{238}\text{U} \text{ age}) / (^{207}\text{Pb}^*/^{206}\text{Pb}^* \text{ age}) \times 100$ . All errors are quoted as  $1\sigma$  level.



**Figure 3** | Rare earth element distribution patterns for the two zircons. Chondrite values are from McDonough and Sun<sup>55</sup>.

[Ti] grains (especially grain #8) suggest a crystallization condition different from the common Jack Hills zircons.

The  $\delta^{18}\text{O}$  value (7.2‰) of the core of grain #8 is similar to the highest values for the Jack Hills magmatic zircons (Fig. 6; Table S4), and is higher than the mantle-like magmatic zircon range ( $5.3 \pm 0.6\%$ , 2SD)<sup>38</sup>. This implies that incorporation of altered crustal material into the magma source, or isotopic exchange of the protoliths with surface water occurred at 4150 Ma ago, which is consistent with previous conclusions<sup>4,9,15,38–40</sup>. The core of grain #8 may have been formed in a granitoid from the melting of supracrustal sediments as Jack Hills zircons, and its high temperature from high-[Ti] indicates a water-free (dry) melting condition that has not been found from Jack Hills zircons.

Oxygen fugacity calculations based on Ce/Ce\* anomalies (see equation (2) in the supplementary files) have been used to constrain the oxidation state of early continental crust<sup>33,40,41</sup>. Note the calculations are mainly controlled by [Ti], [La], [Ce], [Pr] and Ti-in-zircon thermometer, and thus the uncertainty of  $\log f\text{O}_2$  is constrained by the uncertainties of these factors. The two studied grains show large positive Ce/Ce\* anomalies (Table S5; Fig. 3). Two analyses (#TE8.1 and #TE8.5) of the grain #8 core give Ce/Ce\* of 65 and 19, respectively, corresponding to  $\log f\text{O}_2$  of  $-5.3$  ( $\Delta\text{FMQ} + 7.3$ ) and  $-9.7$  ( $\Delta\text{FMQ} + 2.8$ ) at  $910^\circ\text{C}$  (Table S2). The two  $\log f\text{O}_2$  estimates overlap within uncertainty (Fig. 5) and their mean value ( $\Delta\text{FMQ} + 5$ ) is higher than most of published crust-derived Jack Hills zircons (Fig. 5). Although the oxygen fugacity estimates are based on many

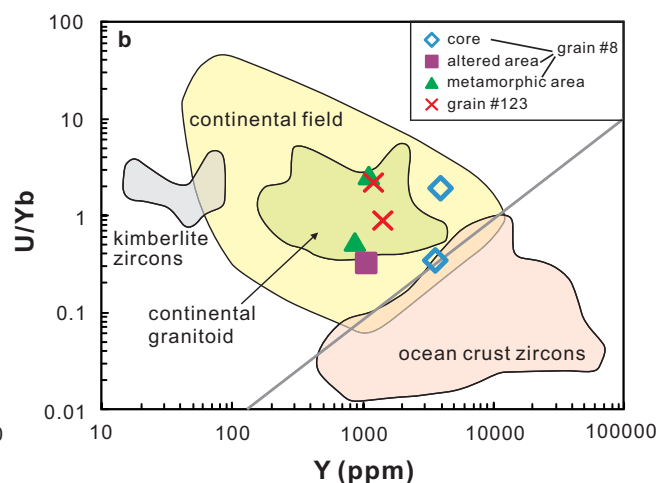
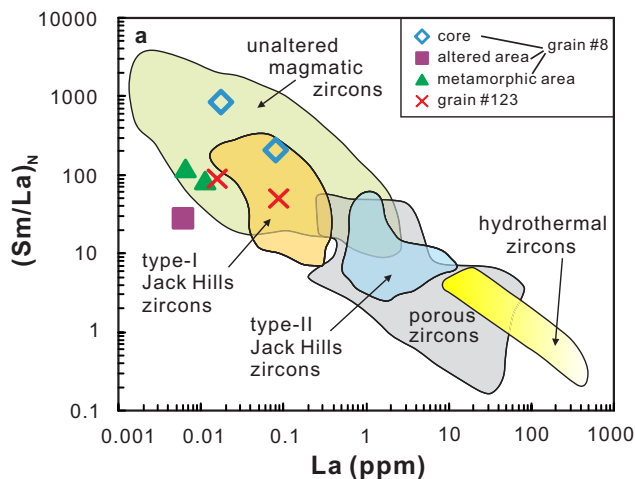


**Figure 4** |  $(\text{Sm}/\text{La})_N$  versus La (a) and  $\text{U}/\text{Yb}$  versus Y (b) plots for the analyses from the two old zircons of southern China. The areas for continental zircons, modern ocean crust zircons, continental granitoid zircons, kimberlite zircons, porous zircons, Jack Hills zircons and hydrothermal zircons are recited from Bouvier et al.<sup>52</sup>.

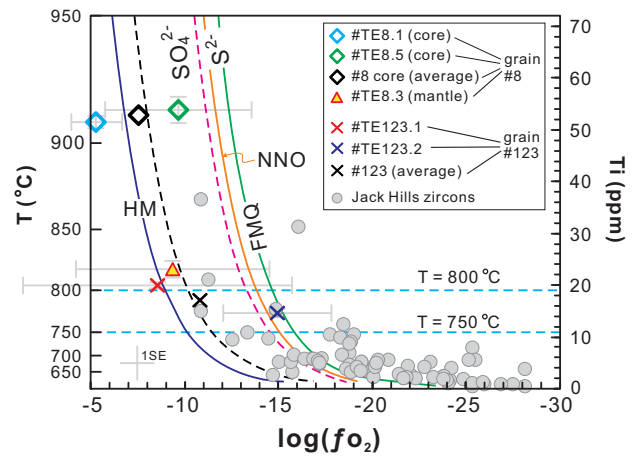


**Figure 5** | Oxygen fugacity ( $f\text{O}_2$ ) versus Ti concentration and calculated temperature by the titanium in zircon thermometer<sup>26,40</sup>. This plot is made based on a compilation (Table S5) of seventy-three  $>3800$  Ma zircons. The temperatures were calculated assuming unit activities of  $\text{TiO}_2$  and  $\text{SiO}_2$  and no pressure correction. Reaction curves of  $f\text{O}_2$  buffer assemblages (HM, hematite–magnetite; NNO, Ni–NiO; FMQ, quartz–fayalite–magnetite) and the boundary between  $\text{SO}_4^{2-}$  and  $\text{S}^{2-}$  predominance in silicate magmas (dashed line) are from Chou<sup>42</sup> and Wallace and Carmichael<sup>56</sup> respectively. The black dashed curve represents the oxygen fugacity shown by the two average analyses from the magmatic zonation of the two grains.

assumptions<sup>41,42</sup>, comparisons at same assumptions are still meaningful in particular for the rare Hadean zircons. The Ce/Ce\* anomalies of the two core analyses of grain #8 are just within the range of published Hadean zircon data<sup>33</sup> (Table S5), suggesting that the high T is the major cause for the high  $\log f\text{O}_2$  according to the equations of Ti-in-zircon thermometry<sup>26,27</sup> and oxygen fugacity<sup>41,42</sup>. Earth's earliest atmosphere had no significant free oxygen because of the absence of photosynthetic prokaryotic organisms, although the early mantle had similar oxygen fugacity as Archean and modern times<sup>40</sup>. The high- $\log f\text{O}_2$  melt for the grain #8 should generate from melting of crustal rocks which originally formed from locally mantle-derived high- $\log f\text{O}_2$  melt which has not been found in Jack Hills zircons yet. This suggests that the oxygen fugacity of early mantle may be heterogeneous.

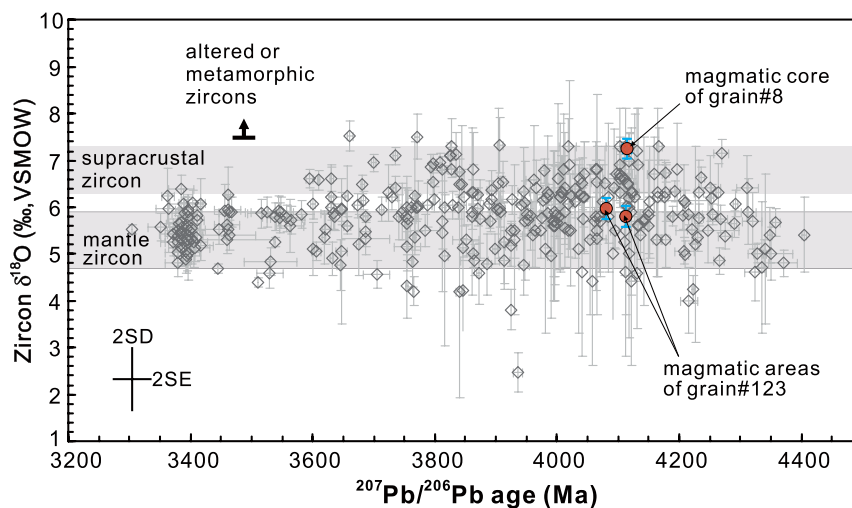


**Figure 6** | A compilation showing the distribution of  $^{207}\text{Pb}/^{206}\text{Pb}$  age versus  $\delta^{18}\text{O}$  for the published analyses on  $>3300$  Ma zircons and the magmatic areas of the two grains of this study. The value for mantle-like zircon ( $5.3 \pm 0.6\text{‰}$ , 2SD) is from the ref. 19. This plot is made on a compilation (Table S4) of 339 magmatic zircons. Only con% between 80% and 120% are included when multiple isotopic ages were provided. The analyses with  $\delta^{18}\text{O}$  errors (2SD) bigger than 1.8 were rejected. Detailed rules in data filtration can be seen in the notes of Supplementary Table S3.

The early earth crust may be heterogeneous as revealed by the variations in Hf, Li and O isotopes in Jack Hills Hadean zircons<sup>3,5,9,15,36,43</sup>, multiple age domains within single zircon grains<sup>44</sup>, and possible heavy bombardment epoch or early earth<sup>45</sup>. Based on the aforementioned discussion, the two 4100 Ma zircon grains (especially grain #8) from southern China are distinct from the published Jack Hills zircons in their high [Ti] and  $\log f\text{O}_2$ . Although a few published Jack Hills zircons showed complexity in CL texture, the pre-3.6 Ga multiple (possibly three episodes according to CL and U-Pb dating results) overgrowths of grain #8 and the 4070–4060 Ma metamorphic mantle are unusual in comparison to Jack Hills zircons. Two possibilities can be addressed for the origins of the two 4100 Ma zircon grains from southern China. Perhaps they were derived from a source area in Western Australia that differed from that of the Jack Hills zircons, or alternatively they could be from a different landmass never attached to the Yilgarn Craton of Western Australia. Further U-Pb dating on other detrital zircons of the studied sample and comparisons with the U-Pb age patterns of Western Australia will be useful way to distinguish them. If the second possibility is correct, Hadean landmasses may have been more widespread than previously known. Either way, the existence of high-[Ti]- $\delta^{18}\text{O}$ -[Ce] zircon and the possible dry melting at ca. 4100 Ma and its 4070–4060 Ma metamorphism suggest diverse tectonic regimes of the Hadean crust.

It should be noted that all four known  $>4050$  Ma zircons dated by SIMS from China (including this work and the two xenocrysts from Tibet and North Qinling Belt<sup>20,21</sup>) are from Phanerozoic sedimentary/volcanic rocks, which is different from the Australia, Greenland and Canada localities where ancient zircons were found in Archean rocks. In addition, rare 3900–4020 Ma detrital zircons were also found in Neoproterozoic and Paleozoic sediments in southern China<sup>46,47</sup> and in Late Devonian sediments in Hexi Corridor of north-western China<sup>48</sup> using laser ablation-ICP-MS method. The sporadic occurrence of Hadean to Early Archean zircons in young sediments in China shows that the Hadean zircons can survive multi-stage crustal recycling. Compared to the other reported  $>4050$  Ma zircons outside Australia, finding two old grains out of 214 zircons of one sample represents a high proportion (nearly 1%) and suggests that more  $>4100$  Ma zircons can be found. Additional U-Pb dating on the detrital zircons in the Longquan area of the Cathaysia Block is necessary to evaluate whether the unusual geochemistry of Hadean

zircons in this study is representative and to help constrain the earliest crustal evolution.

## Conclusions

Two  $\sim 4100$  Ma detrital zircons were found in a Paleozoic quartzite from the Longquan area of southern China. One zircon shows normal magmatic oscillatory zonation in CL and constant mantle-like oxygen isotopes ( $\delta^{18}\text{O} = 5.8\text{--}6.0\text{‰}$ ). The other zircon grain has a  $\sim 4100$  Ma magmatic core surrounded by three  $>3600$  Ma overgrowths, especially a 4070–4060 Ma metamorphic rim. The magmatic core is distinct in its elevated  $\delta^{18}\text{O}$  (7.2‰), high titanium concentration (53 ppm) and a calculated high oxygen fugacity ( $\Delta\text{FMQ} + 5$ ) and crystallization temperature (910°C), suggesting a granitoid-like source generated from dry remelting of partly oxidizing supracrustal sediments altered by surface waters. The unusual melting condition and the immediately following  $\sim 4070$  Ma metamorphism recorded in zircon possibly provide new evidence for diversity of the Earth's earliest continental crust and more ancient zircons other than Western Australia as well as other isotopic and geochemical investigations are necessary to understand the earliest crustal evolution of the Earth.

## Methods

After crushing and grinding, zircons were separated by heavy liquid and magnetic techniques. They were mounted in epoxy with the standard TEMORA 1 ( $^{206}\text{Pb}/^{238}\text{U}$  age = 417 Ma<sup>49</sup>) and polished to mid-section. Detailed cathodoluminescence (CL) images were made for each surface of analysis (Supplementary Fig. DR3). U-Th-Pb zircon analyses were performed on the SHRIMP II ion microprobe at the Beijing SHRIMP center, Chinese Academy of Geological Sciences, following standard operating techniques<sup>14,50</sup>. There are two dating sessions. Four U-Th-Pb isotope analyses (session-1; Table 1) were initially made for each grain (ion beam  $\sim 30$   $\mu\text{m}$  dia.) on surface-1 (Fig. DR3a–d).

After the session-1 dating, the mount was ground lightly and repolished to remove the SIMS pits. Further CL and SEM imaging (surface-2; Fig. DR3e–j) were performed for oxygen isotope and trace element analyses. Oxygen isotope ratios and trace element compositions were analyzed on surface-2 using the CAMECA IMS-1280 ion microprobe in the WiscSIMS Laboratory, UW-Madison, with detailed analytical conditions and data reduction procedures reported elsewhere<sup>51,52</sup>. Oxygen isotopes were analyzed (ion beam  $\sim 8 \times 9$   $\mu\text{m}$ ) with a zircon KIM-5 ( $\delta^{18}\text{O} = 5.09\text{‰}$  VSMOW)<sup>53</sup> as standard. A  $^{133}\text{Cs}^+$  primary ion beam (20 kV total impact voltage, 1.9–2.2 nA) was focused to an area of  $8 \times 9$   $\mu\text{m}$  on the sample surface. Total analytical time per spot was about 4 minutes: including pre-sputtering (10 s), automatic retuning of the secondary beam (120 s), and analysis (80 s). Trace element analyses were performed directly on the same pits as  $\delta^{18}\text{O}$  (beam size  $\sim 10 \times 12$   $\mu\text{m}$ ) at WiscSIMS in single collector mode by axial electron multiplier using magnetic peak switching. Zircon 91500 and NBS610 glass were used as standards following the



method of Page et al.<sup>32</sup> and Fu et al.<sup>54</sup>. A primary  $^{16}\text{O}^-$  beam with a current of 2.5 nA and a total impact energy of 23 kV was defocused to a  $10 \times 12 \mu\text{m}$  spot. An energy offset of 40 eV was applied and the mass resolving power was set at 5000. All analyses consisted of 100 s pre-sputtering, 80 s for centering ions to the field aperture using the  $^{30}\text{Si}^+$  signal followed by seven mass scan cycles for detection of trace element signals, with total analytical time about 24 minutes. Only the last 5 cycles were integrated; the first two cycles were used to stabilize the magnet. After analysis, each pit was imaged by SEM (Scanning electron microscope). No oxygen or trace element analyses have unusual pits and no cracks or inclusions were found in the pits.

The session 2 (Table 1) U–Pb dating analyses were made after oxygen isotope and trace element analysis at the Beijing SHRIMP center. Zircons were reground and repolished to remove all previous analytical pits; the grains were then re-imaged by CL (surface-3; Fig. DR3k–n). Care was taken to locate new analytical sites away from identifiable cracks and the primary ion beam size was adjusted to about 15–20  $\mu\text{m}$  to avoid overlapping of different zones seen by CL. This proved partially successful, with four of six analyses obtained from each grain showing better than 89% concordance (Table 1).

- O'Neil, J., Carlson, R. W., Francis, D. & Stevenson, R. K. Neodymium-142 evidence for Hadean mafic crust. *Science* **321**, 1828–1831 (2008).
- Roth, A. S. G. et al. Inherited  $^{142}\text{Nd}$  anomalies in Eoarchean protoliths. *Earth Planet. Sci. Lett.* **361**, 50–57 (2013).
- Cavosie, A. J., Valley, J. W. & Wilde, S. The oldest terrestrial mineral record: a review of 4400 to 4000 Ma detrital zircons from Jack Hills, Western Australia. *Developments in Precambrian Geology* **15**, 91–111 (2007).
- Harrison, T. M. The Hadean crust: evidence from >4 Ga zircons. *Annu. Rev. Earth Planet. Sci.* **37**, 479–505 (2009).
- Kemp, A. I. S. et al. Hadean crustal evolution revisited: new constraints from Pb–Hf isotope systematics of the Jack Hills zircons. *Earth Planet. Sci. Lett.* **296**, 45–56 (2010).
- Ushikubo, T. et al. Lithium in Jack Hills zircons: evidence for extensive weathering of Earth's earliest crust. *Earth Planet. Sci. Lett.* **272**, 666–676 (2008).
- Bowring, S. A. & Housh, T. The Earth's early evolution. *Science* **269**, 1535–1540 (1995).
- Harrison, T. M. & Schmitt, A. K. High sensitivity mapping of Ti distributions in Hadean zircons. *Earth Planet. Sci. Lett.* **261**, 9–19 (2007).
- Harrison, T. M., Schmitt, A. K., McCulloch, M. T. & Lovera, O. M. Early ( $\geq 4.5$  Ga) formation of terrestrial crust: Lu–Hf,  $\delta^{18}\text{O}$ , and Ti thermometry results for Hadean zircons. *Earth Planet. Sci. Lett.* **268**, 476–486 (2008).
- Kamber, B. S., Collerson, K. D., Moorbath, S. & Whitehouse, M. J. Inheritance of Early Archaean Pb-isotope variability from long-lived Hadean protocrust. *Contrib. Mineral. Petrol.* **145**, 25–46 (2003).
- Kamber, B. S., Whitehouse, M. J., Bolhar, R. & Moorbath, S. Volcanic resurfacing and the early terrestrial crust: zircon U–Pb and REE constraints from the Isua Greenstone Belt, southern West Greenland. *Earth Planet. Sci. Lett.* **240**, 276–290 (2005).
- Kramers, J. D. Hierarchical Earth accretion and the Hadean Eon. *J. Geol. Soc. London* **164**, 3–17 (2007).
- Shirey, S. B., Kamber, B. S., Whitehouse, M. J., Mueller, P. A. & Basu, A. R. A review of the isotopic and trace element evidence for mantle and crustal processes in the Hadean and Archean: implications for the onset of plate tectonic subduction. *GSA Special Paper* **440**, 1–29 (2008).
- Compston, W. & Pidgeon, R. T. Jack Hills, evidence of more very old detrital zircons in Western Australia. *Nature* **321**, 766–769 (1986).
- Wilde, S. A., Valley, J. W., Peck, W. H. & Graham, C. M. Evidence from detrital zircons for the existence of continental crust and oceans on the Earth 4.4 Gyr ago. *Nature* **409**, 175–177 (2001).
- Wyche, S., Nelson, D. R. & Riganti, A. 4350–3130 Ma detrital zircons in the Southern Cross Granite–Greenstone Terrane, Western Australia: implications for the early evolution of the Yilgarn Craton. *Australia J. Earth Sci.* **51**, 31–45 (2004).
- Holden, P. et al. Mass-spectrometric mining of Hadean zircons by automated SHRIMP multi-collector and single-collector U/Pb zircon age dating: the first 100,000 grains. *Inter. J. Mass Spectr.* **286**, 53–63 (2009).
- Mojzsis, S. J. & Harrison, T. M. Establishment of a 3.83-Ga magmatic age for the Akilia tonalite (southern West Greenland). *Earth Planet. Sci. Lett.* **202**, 563–576 (2002).
- Iizuka, T. et al. 4.2 Ga zircon xenocryst in an Acasta gneiss from northwestern Canada: evidence for early continental crust. *Geology* **34**, 245–248 (2006).
- Duo, J., Wen, C. Q., Guo, J. C., Fan, X. P. & Li, X. W. 4.1 Ga old detrital zircon in western Tibet of China. *Chinese Sci. Bull.* **52**, 23–26 (2007).
- Diwu, C. R. et al. In situ U–Pb geochronology of Hadean zircon xenocryst (4.1 ~ 3.9 Ga) from the western of the Northern Qinling Orogenic Belt. *Acta Petrol. Sin.* **26**, 1171–1174 (2010).
- Kusiak, M. A., Whitehouse, M. J., Wilde, S. A., Nemchin, A. A. & Clark, C. Mobilization of radiogenic Pb in zircon revealed by ion imaging: implications for early Earth geochronology. *Geology* **41**, 291–294 (2013).
- Rubatto, D. Zircon trace element geochemistry: partitioning with garnet and the link between U–Pb ages and metamorphism. *Chem. Geol.* **184**, 123–138 (2002).
- Corfu, F., Hanchar, J. M., Hoskin, P. W. O. & Kinny, P. Atlas of Zircon Textures. *Rev. Mineral. Geochem.* **53**, 469–500 (2003).
- Cavosie, A. J., Wilde, S. A., Liu, D. Y., Weiblen, P. W. & Valley, J. W. Internal zoning and U–Th–Pb chemistry of Jack Hills detrital zircons: a mineral record of early Archean to Mesoproterozoic (4348–1576 Ma) magmatism. *Precambrian Res.* **135**, 251–279 (2004).
- Watson, E. B. & Harrison, T. M. Zircon thermometer reveals minimum melting conditions on earliest Earth. *Science* **308**, 841–844 (2005).
- Watson, E. B., Wark, D. A. & Thomas, J. B. Crystallization thermometers for zircon and rutile. *Contrib. Mineral. Petrol.* **151**, 413–433 (2006).
- Nutman, A. P. Comment on “Zircon thermometer reveals minimum melting conditions on earliest Earth”. *Science* **311**, 779b (2006).
- Fu, B. et al. Ti-in-zircon thermometry: applications and limitations. *Contrib. Mineral. Petrol.* **156**, 197–215 (2008).
- Hofmann, A. E., Valley, J. W., Watson, E. B., Cavosie, A. J. & Eiler, J. M. Sub-micron scale distributions of trace elements in zircon. *Contrib. Mineral. Petrol.* **158**, 317–335 (2009).
- Hiess, J., Nutman, A. P., Bennett, V. C. & Holden, P. Ti-in-zircon thermometry applied to contrasting Archean metamorphic and igneous systems. *Chem. Geol.* **247**, 323–338 (2008).
- Page, F. Z. et al. Zircons from kimberlite: new insights from oxygen isotopes, trace elements, and Ti in zircon thermometry. *Geochim. Cosmochim. Acta* **71**, 3887–3903 (2007).
- Yang, X. Z., Gaillard, F. & Scaillet, B. A relatively reduced Hadean continental crust and implications for the early atmosphere and crustal rheology. *Earth Planet. Sci. Lett.* **393**, 210–219 (2014).
- Watson, E. B. & Harrison, T. M. Response to Comments on “Zircon Thermometer Reveals Minimum Melting Conditions on Earliest Earth”. *Science* **311**, 779 (2006).
- Valley, J. W., Spicuzza, M. J. & Ushikubo, T. Correlated  $\delta^{18}\text{O}$  and [Ti] in lunar zircons: a terrestrial perspective for magma temperatures and water content on the Moon. *Contrib. Mineral. Petrol.*, doi:10.1007/s00410-013-0956-4 (2014).
- Trail, D. et al. Constraints on Hadean zircon protoliths from oxygen isotopes, Ti-thermometry, and rare earth elements. *Geochem. Geophys. Geosys.* **8**, Q06014, doi:10.1029/2006GC001449 (2007).
- Moecher, D. P., McDowell, S. M., Samson, S. D. & Miller, C. F. Ti-in-zircon thermometry and crystallization modeling support hot Grenville granite hypothesis. *Geology* doi:10.1130/G35156.1 (2014).
- Valley, J. W. et al. 4.4 billion years of crustal maturation: oxygen isotopes in magmatic zircon. *Contrib. Mineral. Petrol.* **150**, 561–580 (2005).
- Valley, J. W., Peck, W. H., King, E. M. & Wilde, S. A. A cool early Earth. *Geology* **30**, 351–354 (2002).
- Trail, D., Watson, E. B. & Tailby, N. D. The oxidation state of Hadean magmas and implications for early Earth's atmosphere. *Nature* **480**, 79–82 (2011).
- Trail, D., Watson, E. B. & Tailby, N. D. Ce and Eu anomalies in zircon as proxies for the oxidation state of magmas. *Geochim. Cosmochim. Acta* **97**, 70–87 (2012).
- Chou, I. M. [Oxygen buffer and hydrogen sensor techniques at elevated pressures and temperatures] *Hydrothermal Experimental Techniques* [Ulmer, G. C. & Barnes, H. L. (eds.)] [61–99] (Wiley, Chichester, 1987).
- Nebel, O., Rapp, R. P. & Yaxley, G. M. The role of detrital zircons in Hadean crustal research. *Lithos* **190–191**, 313–327 (2014).
- Trail, D., Mojzsis, S. J. & Harrison, T. M. Thermal events documented in Hadean zircons by ion microprobe depth profiles. *Geochim. Cosmochim. Acta* **71**, 4044–4065 (2007).
- Hartmann, W. K. Megareolith evolution and cratering cataclysm models—Lunar cataclysm as a misconception (28 years later). *Meteorit. Planet. Sci.* **38**, 579–593 (2003).
- Yao, J. L., Shu, L. S. & Santosh, M. Detrital zircon U–Pb geochronology, Hf-isotopes and geochemistry – new clues for the Precambrian crustal evolution of Cathaysia Block, South China. *Gondwana Res.* **20**, 553–567 (2011).
- Wang, D., Wang, X. L., Zhou, J. C. & Shu, X. J. Unraveling the Precambrian crustal evolution by Neoproterozoic basal conglomerates, Jianguan orogen: U–Pb and Hf isotopes of detrital zircons. *Precambrian Res.* **233**, 223–236 (2013).
- Yuan, W., Yang, Z. Y. & Yang, J. H. The discovery of Hadean detrital zircon in Late Devonian strata in Hexi Corridor, Northwest China. *Acta Petrol. Sin.* **28**, 1029–1036 (in Chinese with English abstract) (2012).
- Black, L. P. et al. TEMORA 1: a new zircon standard for Phanerozoic U–Pb geochronology. *Chem. Geol.* **200**, 155–170 (2003).
- Wan, Y. S. et al. Episodic Paleoproterozoic (~2.45, ~1.95 and ~1.85 Ga) mafic magmatism and associated high temperature metamorphism in the Daqingshan area, North China Craton: SHRIMP zircon U–Pb dating and whole-rock geochemistry. *Precambrian Res.* **224**, 71–93 (2013).
- Kita, N. T., Ushikubo, T., Fu, B. & Valley, J. W. High Precision SIMS Oxygen Isotope Analyses and the Effect of Sample Topography. *Chem. Geol.* **264**, 43–57 (2009).
- Bouvier, A. S. et al. Li isotopes and trace elements as a petrogenetic tracer in zircon: insights from Archean TTGs and Sanukitoids. *Contrib. Mineral. Petrol.* **163**, 745–768 (2012).
- Valley, J. W. Oxygen isotopes in zircon. *Rev. Mineral. Geochem.* **53**, 343–385 (2003).
- Fu, B. et al. Distinguishing magmatic zircon from hydrothermal zircon: a case study from the Gidginbung high-sulphidation Au–Ag–(Cu) deposit, SE Australia. *Chem. Geol.* **259**, 131–142 (2009).
- McDonough, W. F. & Sun, S.-S. The composition of the Earth. *Chem. Geol.* **120**, 223–253 (1995).



56. Wallace, P. J. & Carmichael, I. S. E. S speciation in submarine basaltic glasses as determined by measurements of SK $\alpha$  X-ray wavelength shifts. *Am. Mineral.* **79**, 161–167 (1994).

## Acknowledgments

This work was supported by a 973 project of China (2012CB416701), the NSFC (Grant Nos. 41222016, 41202141 and 41002024) and the MLR of China (2014111111-7). WiscSIMS is partly supported by the U.S. NSF (EAR- 0319230, 0744079, 1053466). We thank Beijing SHRIMP center, Brian Hess and Jim Kern for sample preparation, John Fournelle for CL and BSE images at UW-Madison, Mike Spicuzza for early stage sample survey, and John Valley for discussions and reviews of early drafts of this paper.

## Author contributions

G.-F.X. and X.-L.W. contributed equally to idea development and data compilation. X.-L.W. and G.-F.X. wrote the main text. G.-F.X. organized the field work, sample

preparation and the session-1 SHRIMP zircon U-Pb dating. Y.-S.W., Z.-H.C., Y.-J., K.K., U.T. and G.P. carried out part of analyses and discussed the manuscript.

## Additional information

**Supplementary information** accompanies this paper at <http://www.nature.com/scientificreports>

**Competing financial interests:** The authors declare no competing financial interests.

**How to cite this article:** King, G.-F. *et al.* Diversity in early crustal evolution: 4100 Ma zircons in the Cathaysia Block of southern China. *Sci. Rep.* **4**, 5143; DOI:10.1038/srep05143 (2014).



This work is licensed under a Creative Commons Attribution-NonCommercial-ShareAlike 3.0 Unported License. The images in this article are included in the article's Creative Commons license, unless indicated otherwise in the image credit; if the image is not included under the Creative Commons license, users will need to obtain permission from the license holder in order to reproduce the image. To view a copy of this license, visit <http://creativecommons.org/licenses/by-nc-sa/3.0/>